cholera and temperature is first observed to the north of Bangladesh over the Himalayas, where temperature leads cholera increases by 6 months (Fig. 5). The pattern then moves south, though it weakens, as the lag to cholera decreases. Ambient temperatures have also been implicated in the dynamics of diarrhoeal diseases and of *V. cholerae* in the environment in Peru (*5*, *22*), and SSTs have been shown to display a bimodal seasonal cycle similar to that of cholera cases in Bangladesh (*2*, *4*).

Another mediating factor in the ENSO-cholera relation might be the melting of the snowpack in the Himalayas, through its effect on the monsoons, precipitation, and river discharge. This scenario, which remains to be investigated, is suggested by the strong but reduced pattern appearing to the north of Bangladesh (Fig. 5, first and second panels). Floods and droughts can affect not only human interactions with water resources and therefore exposure to the pathogen, but also sanitary conditions and susceptibility to disease.

References and Notes

1. For example, see J. L. Bryden, *Epidemic Cholera in the Bengal Presidency* (Office of the Superintendent of Government Printing, Calcutta, India, 1871).
2. R. R. Colwell, *Science* **274**, 2025 (1996).
3. P. R. Epstein, T. E. Ford, R. R. Colwell, *Lancet* **342**, 1216 (1993).
4. B. Lobitz *et al*., *Proc. Natl. Acad. Sci. U.S.A.* **97**, 1438 (2000).
5. W. Checkley *et al*., *Lancet* **355**, 442 (2000).
6. E. Salazar-Lindo, P. Pinell-Salles, A. Maruy, E. Chea-Woo, *Lancet* **350**, 1597 (1997).
7. D. S. Broomhead and G. P. King, *Physica D* **20**, 217 (1986).
8. R. Vautard and M. Ghil, *Physica D* **35**, 395 (1989).
9. Examples of such responses to seasonal forcing in nonlinear models for disease dynamics can be found in W. M. Schaffer *et al*., in *The Ubiquity of Chaos*, S. Krasner, Ed. (American Association for the Advancement of Science, Washington, DC, 1990), pp. 138–166; I. B. Schwartz and H. L. Smith, *J. Math. Biol*. **18**, 233 (1983); and I. B. Schwartz, *J. Math. Biol*. **30**, 473 (1992).
10. S. Ellner and P. Turchin, *Am. Nat*. **145**, 343 (1995).
11. D. W. Nychka, S. Ellner, A. R. Gallant, D. McCaffrey, *J. R. Stat. Soc. B* **54** 399 (1992).
12. F. Takens, in *Dynamical Systems and Turbulence*, D. Rand and L. S. Young, Eds., *Lecture Notes in Mathematics*, vol. 898 (Springer-Verlag, New York, 1981), pp. 366–381.
13. M. Casdagli, in *Nonlinear Modeling and Forecasting*, M. Casdagli and S. Eubank, Eds. (Addison-Wesley, New York, 1992).
14. To fit f we used the feedforward neural network (FNN) model

$$f(x_1, x_2, \ldots, x_d) = \beta_0 + \sum_{i=1}^{k} \beta_i G\left(\sum_{j=1}^{d} \gamma_{ij} x_j + \mu_i\right) \quad (2)$$

where G is a sigmoid function such as $G(y) = e^y/(1 + e^y)$. Given k and the set of independent variables $(x_1, x_2, \ldots x_d)$, the model parameters $(\beta_i, \gamma_{ij}, \mu_i)$ were estimated by ordinary least squares. Models with different values of k or a different set of x's were compared with a GCV criterion function

$$V_c = \left(\frac{RMS}{1 - p\frac{c}{n}}\right)^2 \quad (3)$$

where p is the number of fitted parameters, and n is the sample size. V_1 is the standard GCV criterion [see G. Wahba, *Spline Models for Observational Data* (Society for Industrial and Applied Mathematics, Philadelphia, 1990)]. We used $c = 2$ based on (*11*). This slight over-penalization of model complexity creates a small bias toward simpler models but greatly reduces the chances of spuriously selecting an overly complex model. The FNN models were fitted with FUNFITS, a suite of S/Fortran functions that run in S-Plus (see www.cgd.ucar.edu/stats/Funfits/).
15. We evaluate the significance of the improvement in fit between a "full" model that incorporates a predictor variable and a "reduced" model that omits the variable. The bootstrap test procedure consists of generating a large number of artificial time series with the reduced model and fitting each of these time series with both the full and reduced models. The artificial time series are generated from the reduced model by adding a vector of randomized residuals to the vector of predictions from the reduced model. In the few cases where the resulting values are negative, we replace them by a lower threshold of 0.1 (equal to the minimum value observed in the data). The improvement in fit between the full and reduced models on the original data is compared to the improvements in fit on the artificial time series, in which any apparent improvement is an artifact of the larger number of parameters and variables in the full model. Let $\Delta_i r^2$ denote the difference in r^2 between the full and reduced models for the ith time series (with $i = 0$ being the original data and $i = 1, 2, \ldots n$ being the artificial data). Let p be the fraction of $\Delta_i r^2$, $i > 0$ values that are larger than $\Delta_0 r^2$. The reduced model is then rejected in favor of the full model at significance level α if $p < \alpha$.
16. See, for example, B. Finkenstädt, M. Keeling, B. T. Grenfell, *Proc. R. Soc. London Ser. B* **265**, 753 (1998).
17. S. A. Klein, B. J. Soden, N. Lau, *J. Clim.* **12**, 917 (1999).
18. Monthly measurements of upper-tropospheric humidity for the period 1979–92 [J. Schmetz, L. Vanderberg, C. Geijo, K. Holmlund, *Adv. Space Res*. **16**, 69 (1995); B. J. Soden and F. P. Bretherton, *J. Geophys. Res*. **101**, 9333 (1996)].
19. Monthly measurements of cloud cover for the period 1983–91 are from the International Satellite Cloud Climatology Project [W. B. Rossow and R. A. Schiffer, *Bull. Am. Meteorol. Soc*. **72**, 2 (1991)].
20. Monthly measurements of top-of-atmosphere absorbed solar radiation for the period 1985–89 are from the Earth Radiation Budget Experiment [E. F. Harrison *et al*., *J. Geophys. Res.* **95**, 18687 (1990)].
21. A supplementary figure is available at *Science* Online at www.sciencemag.org/feature/data/1051490.shl.
22. A. A. Franco *et al*., *Am. J. Epidemiol*. **146**, 1067 (1997).
23. M. Ghil and K. Mo, *J. Atmos. Sci*. **48**, 752 (1991).
24. ———, *J. Atmos. Sci.* **48**, 780 (1991).

25. We thank K. Siddique and G. Fuchs for assistance with the cholera data; R. B. Sack, J. Trantj, and the Office of Global Programs at the National Oceanic and Atmospheric Administration for stimulating this work; B. Soden for the cloud cover and radiation data; and M. A. Rodriguez-Arias for computing assistance. M.P. was supported by a James S. McDonnell Foundation Centennial Fellowship and by The Knut and Alice Wallenbergs Foundation; S.P.E. was supported by a grant from the Mellon Foundation to S.P.E. and N.G. Hairston Jr.; X.R. received partial support from the Commissionat per Universitats i Recerca.

19 April 2000; accepted 6 July 2000

Myotonic Dystrophy in Transgenic Mice Expressing an Expanded CUG Repeat

Ami Mankodi,[1] Eric Logigian,[1] Linda Callahan,[2] Carolyn McClain,[1] Robert White,[1] Don Henderson,[1] Matt Krym,[1] Charles A. Thornton[1]*

Myotonic dystrophy (DM), the most common form of muscular dystrophy in adult humans, results from expansion of a CTG repeat in the 3′ untranslated region of the *DMPK* gene. The mutant *DMPK* messenger RNA (mRNA) contains an expanded CUG repeat and is retained in the nucleus. We have expressed an untranslated CUG repeat in an unrelated mRNA in transgenic mice. Mice that expressed expanded CUG repeats developed myotonia and myopathy, whereas mice expressing a nonexpanded repeat did not. Thus, transcripts with expanded CUG repeats are sufficient to generate a DM phenotype. This result supports a role for RNA gain of function in disease pathogenesis.

Myotonic dystrophy (DM, prevalence 1 in 7400 live births) is characterized by dominantly inherited muscle hyperexcitability (myotonia), progressive myopathy, cataracts, defects of cardiac conduction, neuropsychiatric impairment, and other developmental and degenerative manifestations (*1*). This complex phenotype results from the expansion of a CTG repeat in the 3′ untranslated region (3′UTR) of the *DMPK* gene, which encodes a serine-threonine protein kinase (*2*). The transcripts from the mutant allele are retained in the nucleus (*3, 4*), and levels of DMPK protein are correspondingly reduced (*5*). The expanded repeat also changes the structure of adjacent chromatin (*6*) and silences the expression of a flanking gene (*7, 8*), *SIX5*, which encodes a transcription factor.

The effects on DMPK and SIX5 expression may account for particular aspects of the DM phenotype. *Dmpk* knockout mice have reduced force generation in skeletal muscle (*9*) and ab-

[1]Department of Neurology, [2]Department of Neurobiology and Anatomy, School of Medicine and Dentistry, University of Rochester, Box 673, 601 Elmwood Avenue, Rochester, NY 14642, USA.

*To whom correspondence should be addressed. E-mail: charles_thornton@urmc.rochester.edu

normal cardiac conduction (*10*), which suggests that loss of DMPK function may contribute to the muscle weakness and cardiac disease in DM. *Six5* knockout mice have an increased frequency of cataracts (*11, 12*), suggesting that loss of *SIX5* function underlies the development of cataracts in DM. However, neither *Dmpk* nor *Six5* knockout mice have reproduced the myotonia and progressive myopathy (*9, 11, 13*) that are the most characteristic and severe features of the disease. This suggests a species difference in the requirement for SIX5 or DMPK, or the existence of another independent effect of the expanded repeat.

We investigated the possibility that the pathogenic effect of the DM mutation is mediated by the mutant mRNA—in other words, that the nuclear accumulation of expanded CUG repeats is toxic to muscle fibers. This possibility was suggested by the unusual location (3′ noncoding sequence) of the mutation, the retention of mutant *DMPK* mRNA in muscle nuclei (*3*), evidence that expanded CUG repeats form extended hairpins (*14, 15*), and the observation that transcripts with expanded CUG repeats inhibit the differentiation of myogenic cells in tissue culture (*16*). We used a genomic fragment containing the human skeletal actin (*HSA*) gene (*17*) to express an untranslated CUG repeat in the muscle of transgenic mice. An expanded (~250 repeats) or nonexpanded (5 repeats) CTG repeat was inserted in the final exon of the *HSA* gene, midway between the termination codon and the polyadenylation site (Fig. 1A) (*18*). This placement is similar to the relative position of the CTG repeat within the human *DMPK* gene, but the repeat tract is shorter than the highly expanded alleles (1 to 4000 CTG repeats) in DM skeletal muscle (*19*). Except for the repeat, the *HSA* constructs are devoid of sequences from the DM locus. Transgenic mice expressing a similar *HSA* fragment without the added CTG repeat have neither increased actin content nor abnormal muscle histology (*20, 21*), despite having increased levels of actin mRNA. (Human and murine skeletal actin have the same amino acid sequence.)

We obtained seven lines of transgenic mice expressing the long repeat (LR) and five expressing the short repeat (SR) (Fig. 1B and Table 1) (*22*). The transgene was expressed only in skeletal muscle (*23*). Some of the mice from the HSA^{LR} lines carrying the highest number of transgene copies (LR20a and LR21) showed silencing of the transgene. The expanded CTG repeats were fully transcribed, as shown by the appropriate increase in the length of the HSA^{LR} mRNA and its hybridization with a $(CAG)_{10}$ probe (Fig. 1C).

Analysis of the HSA^{LR} mRNA by Northern blot (Fig. 1C) and sequencing of HSA^{LR} cDNAs revealed that the long-repeat transcripts were fully spliced and polyadenylated, and that the actin coding sequence was intact (*24*). A variable amount of the *HSA* mRNA in line L32a was shortened (Fig. 1B) because of activation of cryptic splice sites in the 3′UTR, which results in the excision of the CUG repeat tract and 72 nucleotides (nt) of flanking sequence in an intron (*25*). This splice event was also detected at low levels by reverse transcription–polymerase chain reaction (RT-PCR) in other long-repeat lines, but not in lines with short repeats.

The phenotype of mice in line LR32a was analyzed most extensively because the expression level of the long-repeat transgene was high and silencing was infrequent. These mice showed normal weight gain and histology of nonmuscle tissue, but after weaning they had a mortality of 41% by 44 weeks (versus <5% in nontransgenic or HSA^{SR} mice). Necropsy did not reveal the cause of death. In DM, cardiac arrhythmia is the second leading cause of death. Although we did not detect HSA^{LR} expression in the heart, the possibility of regional, low-level, or transient expression has not been excluded. There was no evidence of muscle weakness in LR32a mice at 6 months of age (*26*).

Electromyography in HSA^{LR} lines revealed high-frequency (50 to 200 Hz) runs of muscle action potentials that continued for 1 to 20 s after insertion or repositioning of the recording electrode (Fig. 1E) (*27*). These repetitive discharges waxed and waned in frequency and amplitude, as is typical of myotonia in DM. Myotonic discharges were observed in six of seven lines that expressed long repeats, but not in short-repeat or wild-type mice (Table 1). The long-repeat mice also showed abnormal hind-

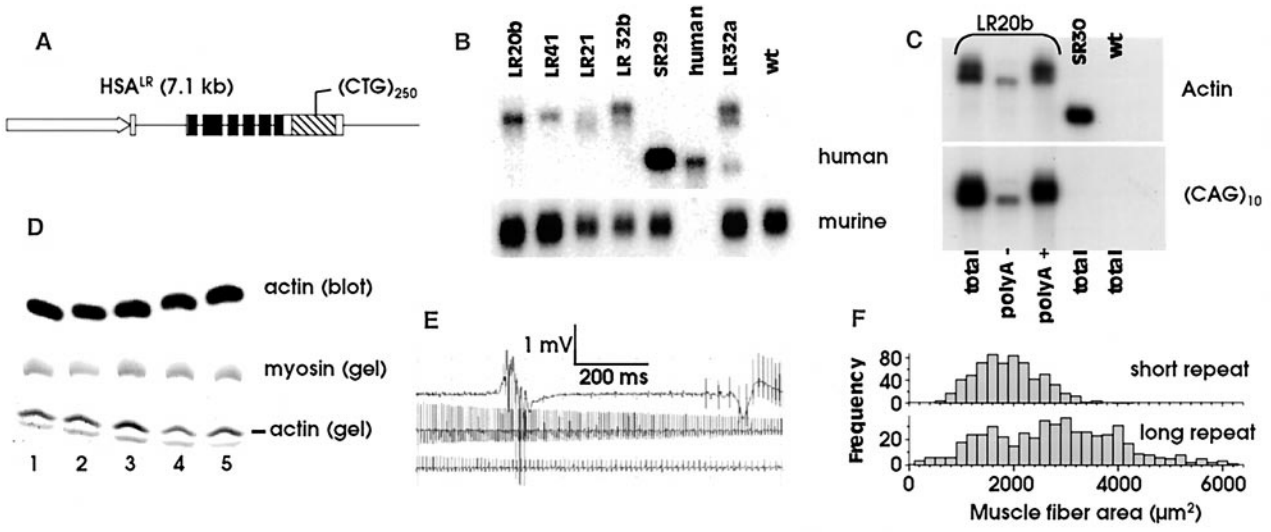

Fig. 1. Expression of *HSA* transgenes. (**A**) Diagram of *HSA* construct. Filled boxes are the *HSA* coding sequence. (**B**) Analysis of skeletal actin expression in vastus (quadriceps) muscle by Northern blot using human- or murine-specific actin cDNA probes. The human probe detects transgene output. The murine probe is a load standard that detects endogenous actin mRNA. The human RNA was isolated from a surgical sample and is partially degraded. (**C**) Northern blot of total cellular RNA (3 μg), nonpolyadenylated RNA (3 μg), and polyadenylated RNA (100 ng) with human-specific skeletal actin cDNA probe or $(CAG)_{10}$ oligonucleotide. A small proportion of the HSA^{LR} RNA is present in the nonpolyadenylated [polyA(−)] fraction. It is unclear whether these polyA(−) transcripts are the result of incorrect formation or degradation of the 3′ end, or of incomplete fractionation. (**D**) Analysis of actin protein in gastrocnemius muscle by protein immunoblot (upper panel) or Coomassie-stained polyacrylamide gels (lower panels) does not show aberrant migration of actin or increased actin mass in short-repeat line SR29 (lane 3) or long-repeat line LR32a (lanes 4 and 5) compared with nontransgenic littermates (lanes 1 and 2). (**E**) Myotonic discharge in paraspinal muscle of a mouse from line LR32a, elicited by brief movement of the EMG electrode. (**F**) Frequency histogram of cross-sectional area shows increased variability of muscle fiber size in long-repeat line LR329 relative to short-repeat line SR24.

limb posture when they initiated movement after a period of inactivity or when they were suspended by the tail. Myotonia was present in *HSA*^{LR} mice as early as 4 weeks of age, when the muscles had a normal histologic appearance. These observations indicate that *HSA*^{LR} mice have a true myotonic disorder, rather than nonspecific hyperexcitability associated with muscle necrosis.

Mice that expressed the long-repeat transgene developed histologically defined myopathy, whereas those expressing short repeats did not (Fig. 2 and Table 1) (*28*). Six of seven lines expressing long repeats showed a consistent pattern of muscle histopathology, including increases in central nuclei and ring fibers and variability in fiber size (Fig. 1F). Higher levels of *HSA*^{LR} expression were associated with more severe pathology (Table 1). Although abundant central nuclei, variability in fiber size, and ring fibers can each be observed in other disorders, this constellation of features in the absence of muscle fiber necrosis is suggestive of DM (*29*). In addition, mice in line LR32a had up-regulated the activity of succinate dehydrogenase (Fig. 2H) and cytochrome oxidase (*23*), a characteristic feature of oxidative muscle fibers. This alteration may have been triggered by the repetitive myotonic discharges, because a similar oxidative transformation in the muscle of *Clcn1*^{Adr} myotonic mice is reversible with anti-myotonia treatment (*30*). The proportion of oxidative fibers is also increased in human DM (*31*).

To quantitate the changes in myonuclear number and location, we performed morphometry with antibodies to laminin to outline the basement membrane of muscle fibers (Fig. 2, E and F) (*32*) and to distinguish muscle nuclei from the nuclei of interstitial cells. Relative to mice expressing short repeats, mice in line LR32a had more than twice the number of nuclei per muscle fiber and a much higher proportion of central nuclei (Table 2). In human DM there is a similar up-regulation of myonuclear number and a marked increase in central nuclei (*33*).

The intracellular location of expanded CUG repeats was determined by fluorescence in situ hybridization (FISH) (*34*). The long-repeat transcripts were retained in the nucleus in multiple discrete foci (Fig. 2G) reminiscent of those seen in fibroblasts and myoblasts from DM patients (*3*). Because the expanded CUG repeat is the only sequence shared by the *HSA*^{LR} and *DMPK* mRNAs, it appears that this sequence is sufficient to trigger the nuclear retention of a mature mRNA.

These results are consistent with the idea that transcripts with expanded CUG repeats are

Table 1. Characteristics of *HSA* transgenic lines. For relative *HSA* expression levels, +++ is similar to the level of *HSA* mRNA in human skeletal muscle. For electromyography, the number of mice showing myotonia per number examined is shown. "–" indicates lines that were not examined. Histologic analysis and electromyography were performed on mice aged 6 to 14 months, except for lines LR32a and LR41, where seven younger mice (1 to 4 months) were also analyzed. Twenty-two mice in line LR32a had abundant myotonia in all regions examined, and seven had myotonia in paraspinal but not forelimb muscles (hindlimbs were not examined). Six hemizygous LR41 mice did not have myotonia up to 14 months of age, but four homozygous animals all developed myotonia before the age of 4 months. CN, central nuclei; +++ indicates CN in more than 25% of fibers.

Line	Copy number	mRNA level	Myotonia	Muscle histopathology
Wild type	–	–	0/16	Normal (n = 16)
SR05	4	+	–	Normal (n = 2)
SR25	20	++	–	Normal (n = 1)
SR29	6	+++	0/6	Normal (n = 5)
SR30	4	++	0/5	Normal (n = 5)
SR40	2	+++	0/4	Normal (n = 4)
LR11	1	0	0/5	Normal (n = 8)
LR5a	12	0	–	Normal to + CN (n = 2)
LR5b	2	+	0/4	Normal (n = 5)
LR41	1	+	4/10	+ to ++ CN, ring fibers (n = 10)
LR20a	5	0 to +++	4/8	++ to +++ CN, ring fibers, sarcoplasmic masses (n = 16)
LR20b	2	++	6/6	++ CN, ring fibers, rare necrotic fiber (n = 5)
LR21	5	0 to +++	4/4	+ to ++ CN (n = 9)
LR32a	4	++ to +++	29/31	+++ CN, atrophic fibers, ring fibers, sarcoplasmic masses (n = 19)
LR32b	2	++	2/2	++ CN, atrophic fibers, ring fibers (n = 3)

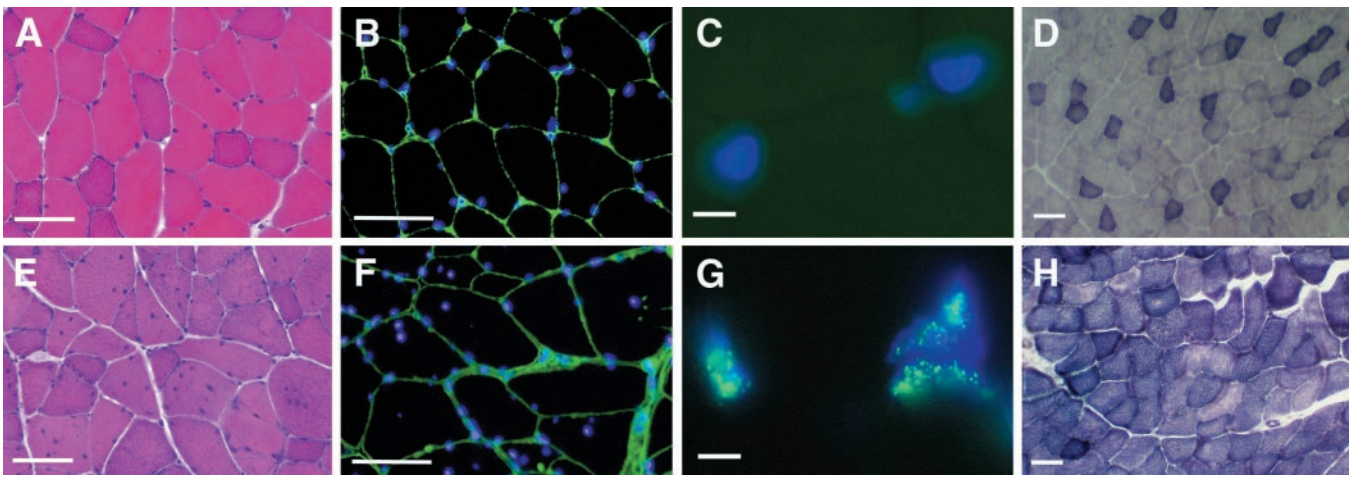

Fig. 2. Muscle histology of short-repeat (line SR29) (**A** to **D**) or long-repeat (line LR32a) (**E** to **H**) transgenic mice. Representative images are transverse frozen sections of vastus muscle obtained from 6-month-old mice. Hematoxylin and eosin–stained muscle is normal in line SR29 (A) but shows increased variability in fiber size, split fibers, and central nuclei in line LR32a (E). Fluorescence microscopy using stains for nuclei (DAPI, blue) and basement membrane (anti-laminin, green) shows increased central and peripheral muscle nuclei in line LR32a (F) compared to line SR29 (B). FISH using CAG repeat oligonucleotide probe shows multiple discrete foci of expanded CUG repeats (green) in muscle nuclei (blue) of line LR32a (G), but not in line SR29 (C). These results are representative of five separate FISH experiments in line LR32a and two experiments in lines LR41 and LR20b. Histochemical stains for succinate dehydrogenase show increased activity and loss of fiber-type distinctions in line LR32a (H) relative to line SR29 (D). Scale bars, 5 μm in (C) and (G), 100 μm in other panels.

Table 2. Morphometric analysis of muscle in *HSA* transgenic lines. Values are means ± SD for measurements of >100 muscle fibers per mouse, $n = 4$ mice per group. *$P < 0.05$, **$P \leq 0.001$.

	Short-repeat SR29	Long-repeat LR32a
Muscle fiber cross-sectional area (μm^2)	1849 ± 329	2710 ± 550*
Muscle nuclei per muscle fiber	0.8 ± 0.14	2.9 ± 0.7**
Number of muscle nuclei per fiber cross-sectional area (mm^2)	450 ± 40	1100 ± 400*
Muscle nuclei that are central (%)	1.4 ± 0.6	38 ± 0.09**

deleterious in muscle fibers. A direct effect by the CTG repeat tract in DNA is unlikely, because HSA^{LR} mice that do not express the mRNA appear normal. An effect by actin protein is unlikely because (i) HSA^{SR} lines had no myopathy or myotonia, (ii) the levels of actin protein were not increased in long- or short-repeat lines (Fig. 1D) (*35*), (iii) mutant actin was not detected (Fig. 1D), (iv) nuclear retention would limit the translation of HSA^{LR} transcripts, and (v) the protein product of the HSA^{LR} mRNA, if it were translated, would be identical to murine skeletal actin. Current formulations for the mechanism of genetic dominance, which posit effects solely at the level of proteins encoded by mutant genes (*36*), may need to be revised.

The mechanism by which transcripts with expanded CUG repeats induce myotonia and muscle degeneration is unclear. Models involving trans-interference with polyadenylation (*37*) or splicing (*38*), sequestration of a CUG binding protein (*39*), or interactions with double-stranded RNA binding proteins (*15*) have been proposed. The deleterious effects of expanded CUG repeats are probably not restricted to skeletal muscle or DM, because expansion of an untranslated CTG repeat in a brain-expressed gene was recently associated with autosomal dominant cerebellar degeneration (*40*).

Muscle wasting and weakness is a frequent feature of DM. HSA^{LR} mice, however, have not developed obvious weakness or muscle wasting by the age of 6 months. It is possible that muscle regeneration and repair can compensate for the myopathy in HSA^{LR} mice. Alternatively, the HSA^{LR} model may be incomplete because of factors related to the CUG repeat (its length, developmental expression, and flanking sequences) or a requirement for other effects of the *DM* mutation, such as deficiency of DMPK or SIX5.

References and Notes

1. P. S. Harper, *Myotonic Dystrophy* (Saunders, London, 1989).
2. J. D. Brook *et al*., *Cell* **68**, 799 (1992).
3. K. L. Taneja, M. McCurrach, M. Schalling, D. Housman, R. H. Singer, *J. Cell Biol.* **128**, 995 (1995).
4. B. M. Davis, M. E. McCurrach, K. L. Taneja, R. H. Singer, D. E. Housman, *Proc. Natl. Acad. Sci. U.S.A.* **94**, 7388 (1997).
5. Y. H. Fu *et al*., *Science* **260**, 235 (1993).
6. A. D. Otten and S. J. Tapscott, *Proc. Natl. Acad. Sci. U.S.A.* **92**, 5465 (1995).
7. T. R. Klesert, A. D. Otten, T. D. Bird, S. J. Tapscott, *Nature Genet.* **16**, 402 (1997).
8. C. A. Thornton, J. P. Wymer, Z. Simmons, C. McClain, R. T. Moxley, *Nature Genet.* **16**, 407 (1997).
9. S. Reddy *et al*., *Nature Genet.* **13**, 325 (1996).
10. C. I. Berul *et al*., *J. Clin. Invest.* **103**, R1 (1999).
11. T. R. Klesert *et al*., *Nature Genet.* **25**, 105 (2000).
12. P. S. Sarkar *et al*., *Nature Genet.* **25**, 110 (2000).
13. G. Jansen *et al*., *Nature Genet.* **13**, 316 (1996).
14. S. Michalowski *et al*., *Nucleic Acids Res.* **27**, 3534 (1999).
15. B. Tian *et al*., *RNA* **6**, 79 (2000).
16. J. D. Amack, A. P. Paguio, M. S. Mahadevan, *Hum. Mol. Genet.* **8**, 1975 (1999).
17. A. Taylor, H. P. Erba, G. E. Muscat, L. Kedes, *Genomics* **3**, 323 (1988).
18. The orientation of the *HSA* fragment in plasmid pHSA.400 (*17*) was reversed. A CTG_{130} fragment was "dimerized" as described (*15*) and inserted at the Bsr GI site in the *HSA* 3′UTR. The construct was sequenced to confirm that all *HSA* introns and exons were intact and that the CTG repeat tract was uninterrupted. For short-repeat constructs, linkers were used to insert five CTG repeats.
19. C. A. Thornton, K. Johnson, R. T. Moxley, *Ann. Neurol.* **35**, 104 (1994).
20. K. J. Brennan and E. C. Hardeman, *J. Biol. Chem.* **268**, 719 (1993).
21. E. Hardeman, personal communication.
22. Transgenic lines were derived and maintained on an FVB/n background. Nine lines of HSA^{LR} mice were segregated from six founders, of which seven expressed the transgene. Six lines of HSA^{SR} mice were segregated from seven founders, of which five expressed the transgene. The length of the expanded repeat varied from 245 to 256 repeats, as determined by PCR with primers that flanked the repeat. The lack of interruptions in the expanded repeat was shown by bidirectional sequencing of the PCR-amplified repeat block in six different HSA^{LR} lines. There was minor intergenerational instability (± up to 20 CTG repeats) in the HSA^{LR} lines. For Northern blots, RNA (3 μg) was probed with human-specific actin probe (nucleotides 1236 to 1385 in GenBank accession no. JOOO68), mouse-specific actin probe (nucleotides 1194 to 1294 in GenBank accession no. M12866), or end-labeled $(CAG)_{10}$ oligonucleotide.
23. A. Mankodi *et al*., data not shown.
24. The *HSA* coding sequence, including all exon boundaries, was amplified from hexamer-primed cDNAs, using two primer sets [nucleotides 11 to 28 (1354 to 1336) or nucleotides 58 to 80 (1280 to 1259), GenBank accession no. J00068] that gave equivalent results. The PCR products were analyzed by gel electrophoresis and dideoxy sequencing.
25. Northern blots using a series of human-specific oligonucleotide probes [three in the actin 3′UTR, one in the 5′UTR, and $(CAG)_{10}$] showed that the shorter *HSA* mRNA lacked the CUG repeat and sequence immediately 3′ to the repeat. An RT-PCR product was generated with primers flanking the missing sequence. The sequence of this product indicated activation of cryptic splice donor and acceptor sites in the *HSA* 3′UTR, 16 nt upstream and 56 nt downstream from the repeat tract (nucleotides 3435 to 3482 in GenBank accession no. M20543). PCR of genomic DNA did not show a similar rearrangement.
26. To measure muscle strength, we adapted the whole-body pulling force procedure (*41*). Force generation (in grams) was 290 ± 50 ($n = 23$) in wild-type, 290 ± 50 ($n = 27$) in short-repeat, and 270 ± 40 ($n = 13$) in long-repeat mice.
27. Electromyography (EMG) was performed under halothane anesthesia using 30-gauge concentric needle electrodes, with sampling of at least three proximal and three distal muscle groups in each forelimb, plus the lumbosacral paraspinals. Hindlimb muscles were spared for histology and RNA isolation. Video clips of EMG recordings are available at www.urmc.rochester.edu/thornton.
28. Frozen muscle sections (10 μm) were stained by standard histologic and histochemical methods, including cytochrome oxidase and succinate dehydrogenase (*29*).
29. V. Dubowitz, *Muscle Biopsy. A Practical Approach* (Bailliere Tindall, London, ed. 2, 1996).
30. J. Reininghaus, E. M. Fuchtbauer, K. Bertram, H. Jockusch, *Muscle Nerve* **11**, 433 (1988).
31. H. Tohgi, A. Kawamorita, K. Utsugisawa, M. Yamagata, M. Sano, *Muscle Nerve* **17**, 1037 (1994).
32. Immunofluorescence was performed on frozen sections (10 μm) of vastus (quadriceps) muscle stained with rabbit polyclonal antibody to laminin (Sigma), Alexa 488–labeled goat secondary antibody to rabbit immunoglobulin G (Molecular Probes), and 33 nM diamidino-2-phenylindole (DAPI). Muscle nuclei (defined as myonuclei plus satellite cell nuclei) were counted and fiber cross-sectional areas were measured using ImagePro-Plus v3.0. Oxidative and glycolytic fibers were not quantified separately, because it was not possible to make fiber type distinctions in HSA^{LR} mice.
33. D. Vassilopoulos and E. M. Lumb, *Eur. Neurol.* **19**, 237 (1980).
34. For FISH, frozen sections (6 μm) of vastus muscle were fixed (73% ethanol, 25% acetic acid, 2% formalin) for 30 min at 4°C, prehybridized for 10 min, hybridized with probe (2 ng/μl) for 2 hours at 37°C in buffer [30% formamide, 2× SSC, 0.02% bovine serum albumin, yeast tRNA (1 mg/ml), and 200 mM vanadate], and washed in 30% formamide and 2× SCC for 30 min at 45°C followed by 1× SCC for 30 min at 22°C. The nuclear counterstain was 33 nM DAPI. The probes were fluorescein 5′ end-labeled $(CAG)_n$ or $(CUG)_n$ 2-*O*-methyl RNA 20-nt oligomers (IDT, Coralville, IA). Specificity was demonstrated by the absence of signal in sections from short-repeat and wild-type muscle on the same slide, or on parallel slides hybridized with sense (CUG) probe.
35. Gastrocnemius muscle (100 mg) was pulverized under liquid nitrogen, homogenized in 10 mM tris-HCl (pH 7.6), 2% SDS, and 2 mM dithiothreitol, and then centrifuged at 12,000 rpm for 10 min at 4°C. For actin quantitation, 8 μg of muscle protein ($n = 3$ in each group) or 0.5 to 2 μg of skeletal acptin (Sigma, for standard curve) was resolved on 5 to 20% gradient polyacrylamide gels, stained with Coomassie blue, and quantified by densitometry. Actin levels (nanograms of actin per microgram of muscle protein) were 170 ± 10 in wild-type, 150 ± 20 in short-repeat, and 150 ± 10 in long-repeat mice. The ratio of actin to myosin (by densitometric volume) was 0.69 ± 0.03 in wild-type, 0.68 ± 0.07 in short-repeat, and 0.61 ± 0.1 in long-repeat mice. Protein immunoblots were probed with actin-specific monoclonal antibody 5C5 (Sigma) at 1:5000.
36. A. O. Wilkie, *J. Med. Genet.* **31**, 89 (1994).
37. J. Wang *et al*., *Hum. Mol. Genet.* **4**, 599 (1995).
38. A. V. Philips, L. T. Timchenko, T. A. Cooper, *Science* **280**, 737 (1998).
39. L. T. Timchenko *et al*., *Nucleic Acids Res.* **24**, 4407 (1996).
40. M. D. Koob *et al*., *Nature Genet.* **21**, 379 (1999).
41. M. S. Hudecki and C. M. Pollina, *Adv. Exp. Med. Biol.* **280**, 251 (1990).

42. We thank L. Kedes for clone pHSA.400, H. Federoff and R. Moxley for discussions, R. Howell and staff in the Transgenic Facility, and R. Tawil and A. Brooks for assistance with image analysis. Supported by the Muscular Dystrophy Association, the Saunders Family Neuromuscular Research Fund, and the Wayne C. Gorrell Jr. Molecular Biology Laboratory. C.A.T. is a Paul Beeson Jr. Physician Faculty Scholar of the American Federation for Aging Research.

25 April 2000; accepted 20 July 2000